Environmental Toxicology and Chemistry—Volume 40, Number 11—pp. 3078–3091, 2021
Received: 12 April 2021 | Revised: 10 May 2021 | Accepted: 27 July 2021

Environmental Toxicology

Sources and Fate of the Antiandrogenic Fluorescent Dye 4-Methyl-7-Diethylaminocoumarin in Small River Systems

Matthias Muschket,[a,*] Werner Brack,[a,b] Pedro A. Inostroza,[c] Liza-Marie Beckers,[a] Tobias Schulze,[a] and Martin Krauss[a]

[a]UFZ–Helmholtz Centre for Environmental Research, Leipzig, Germany
[b]Department of Evolutionary Ecology and Environmental Toxicology, Faculty of Biological Sciences, Goethe University Frankfurt, Frankfurt am Main, Germany
[c]Department of Biological and Environmental Sciences, University of Gothenburg, Gothenburg, Sweden

Abstract: Recently, the potent antiandrogen 4-methyl-7-diethylaminocoumarin (C47) and its potential transformation products 4-methyl-7-ethylaminocoumarin (C47T1) and 4-methyl-7-aminocoumarin (C47T2) were identified as novel environmental contaminants. We assessed for the first time the sources, distribution, and fate of these compounds in aquatic systems using the Holtemme River (Saxony-Anhalt, Germany), which is a hotspot for these contaminants. To this end, wastewater-treatment plant (WWTP) influent and effluent samples, surface water samples over 3 years, and the longitudinal profiles in water, sediment, and gammarids were analyzed. From the longitudinal profile of the river stretch, the WWTP of Silstedt was identified as the sole point source for these compounds in the River Holtemme, and exposure concentrations in the low micrograms per liter range could be recorded continuously over 3 years. Analysis of WWTP influent and effluent showed a transformation of approximately half of the C47 into C47T1 and C47T2 but no complete removal. A further attenuation of the three coumarins after discharge into the river could be largely attributed to dilution, while transformation was only approximately 20%, thus suggesting a significant persistence in aquatic systems. Experimentally derived partitioning coefficients between water and sediment organic carbon exceeded those predicted using the OPERA quantitative structure–activity relationship tools and polyparameter linear free-energy relationships by up to 93-fold, suggesting cation binding as a significant factor for their sorption behavior. Near-equilibrium conditions between water and sediment were not observed close to the emitting WWTP but farther downstream in the river. Experimental and predicted bioaccumulation factors for gammarids were closely matching, and the concentrations in field-sampled gammarids were close to steady state with exposure concentrations in the water phase of the river. *Environ Toxicol Chem* 2021;40:3078–3091. © 2021 The Authors. *Environmental Toxicology and Chemistry* published by Wiley Periodicals LLC on behalf of SETAC.

Keywords: Bioaccumulation; Endocrine-disrupting compounds; Environmental fate; Environmental partitioning; Equilibrium partitioning theory

INTRODUCTION

In a recent study, 4-methyl-7-diethylaminocoumarin (C47) was identified as a potent antiandrogenic compound in the Holtemme River (Saxony-Anhalt, Germany; Muschket et al., 2018). Simultaneously, the two structurally related compounds 4-methyl-7-ethylaminocoumarin (C47T1) and 4-methyl-7-aminocoumarin (C47T2) were found and considered to be likely transformation products of C47 based on the fact that *N*-dealkylation is a commonly observed microbial transformation pathway in the activated sludge of wastewater-treatment plants (WWTPs; Gulde et al., 2016; Figure 1). The antiandrogenic potential of C47 and, to a lesser extent, of C47T1 and C47T2 was not only detected in vitro in the cell-based antiAR-CALUX assay (Di Paolo et al., 2016) but also confirmed for C47 and C47T1 in vivo in spiggin-gfp medaka (Sébillot et al., 2014).

Derivatives of coumarin can be found all over the plant kingdom (Lacy & O'Kennedy, 2004) and are used in various consumer products, such as bathroom air fresheners, because of their olfactory properties. Synthetic coumarin derivatives, particularly if substituted at position 7 with an electron donating group, such as the 7-aminocoumarins, exhibit strong fluorescence and thus are used as fluorescent probes, dyes, and optical

This article includes online-only Supporting Information.

* Address correspondence to matthias.muschket@ufz.de
Published online 29 July 2021 in Wiley Online Library (wileyonlinelibrary.com).
DOI: 10.1002/etc.5181

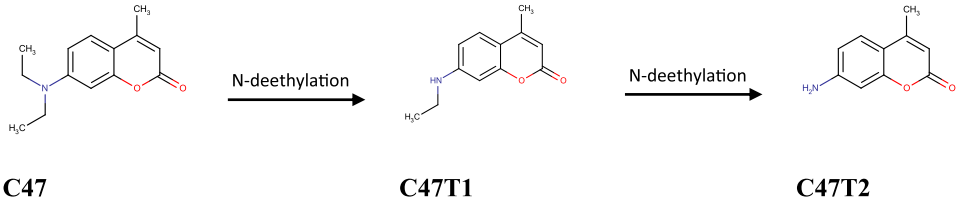

FIGURE 1: Proposed transformation of 4-methyl-7-diethylaminocoumarin (C47) to 4-methyl-7-ethylaminocoumarin (C47T1) and 4-methyl-7-aminocoumarin (C47T2) by consecutive *N*-deethylation.

brighteners (Kitamura et al., 2007). The Chemical Product and Use Category database of the US Environmental Protection Agency (2020) lists 18 different use categories for C47, which include inks, colorants and paints, cracking indicators, lubricants, and use in industry and manufacturing of various products. The European Chemicals Agency (2020) registration dossier states that the volume of C47 produced or imported in Europe amounts to 10 to 100 tons per year and lists its uses in washing and cleaning products, in leather treatment products, and as a paper chemical or dye and textile treatment product or dye.

To the best of our knowledge, the occurrence, distribution, and fate of the three coumarin derivatives C47, C47T1, and C47T2 in the aquatic environment have not been described before in the literature. In the study of Loos et al. (2003), C47 was among the target compounds but could not be detected in surface waters from northern Italy. Krauss et al. (2019) confirmed the presence of C47, C47T1, and C47T2 in the Holtemme River downstream of a WWTP using nontarget screening, with chromatographic peak intensities indicating high concentrations in the micrograms per liter range. These compounds were also detected in an additional six out of 31 sites in the Saale and Mulde catchments at >50-fold lower peak intensities, suggesting that the high abundance in the Holtemme River is related to a specific point source. This river provides the opportunity to study the occurrence, fate, and distribution of these compounds in a real-world aquatic system.

The objective of the present study was to assess sources, distribution, and fate of these compounds in aquatic systems. Specifically, we studied 1) the longitudinal profile of C47, C47T1, and C47T2 in the water phase to unravel sources and transformation; 2) the temporal variation in the water phase over 3 years; and 3) the attenuation in the river and whether C47T1 and C47T2 are formed from C47 during wastewater treatment. Moreover, 4) the distribution among water, sediment, and biota represented by *Gammarus pulex* was studied using experimentally determined partition coefficients as well as software predictions.

MATERIAL AND METHODS

Chemicals and reagents

The reference compounds C47, C47T1, C47T2, carbamazepine, metazachlor ethane sulfonic acid (ESA), ^{1}H-benzotriazole, 4-methyl-^{1}H-benzotriazole, and the isotope-labeled internal standards bezafibrate-d4, atrazine-$^{13}C_3$ and imidacloprid-d4 used for their quantification were obtained from different sources and had a purity of ≥98%. Liquid chromatography–mass spectrometry (LC-MS)–grade methanol, water, ethyl acetate, acetonitrile, and formic acid were obtained from Sigma-Aldrich. Acetone, dichloromethane, and hexane were of LC grade and supplied by Merck, magnesium sulfate and sodium

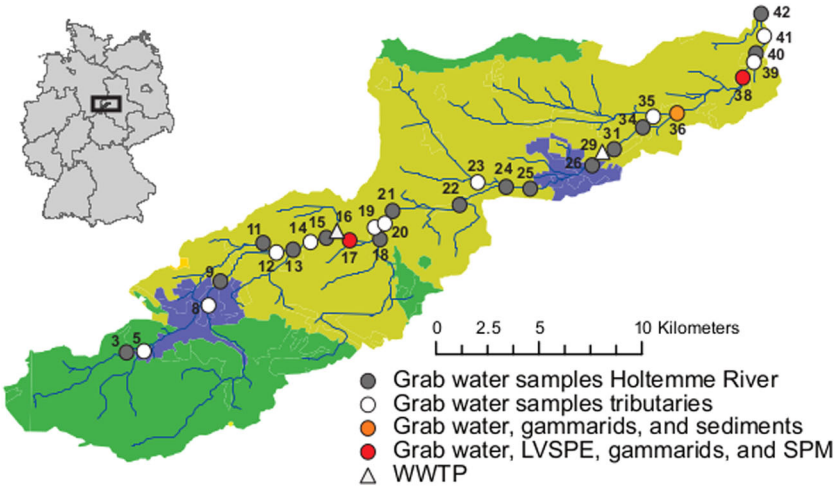

FIGURE 2: Map of the Holtemme River catchment showing sampling sites 3 to 42. Several campaigns detailed in Table 1 were conducted to obtain different types of samples at the sites as shown in the legend. Green areas indicate forests, olive indicates agricultural areas, and blue represents main settlements. The wastewater-treatment plants of Silstedt (site 16) and Halberstadt (site 29) are indicated by triangles. LVSPE = large-volume solid-phase extraction of water; SPM = suspended particulate matter; WWTP = wastewater-treatment plant.

chloride (both of analytical grade) by Sigma-Aldrich, and primary-secondary amine by Agilent.

Study area and sample overview

The Holtemme River is located in Saxony-Anhalt, Germany (Figure 2) and has a length of 47 km, a basin of 282 km^2, and a mean annual discharge of 1.53 m^3/second (period 1983–2015) close to the mouth into the Bode River at 85 meters above sea level (a.s.l.). While its source at 862 meters a.s.l. and upper stretch are located in the near-natural forest in the Harz Mountains national park, its lower stretches are characterized by strong hydromorphological alterations caused by channelization and riparian clear-cutting in a landscape characterized by intense agriculture and settlements.

The river passes through the towns of Wernigerode and Halberstadt and receives effluents from 2 WWTPs, at Silstedt (80 000 population equivalent, average discharge 11 500 m^3/d) serving Wernigerode and the surrounding villages and at Halberstadt (60 000 population equivalents, average discharge 7600 m^3/d). While WWTP Silstedt is connected to a separate sewage collection system, WWTP Halberstadt is fed by a combined sewer system. Both WWTPs are equipped with activated sludge treatment and advanced nitrogen and phosphorus elimination; the hydraulic retention times are approximately 72 hours in Silstedt and 54 hours in Halberstadt under dry weather conditions.

We collected samples in 42 sampling sites along the Holtemme River and some of its tributaries (Figure 2). Water, sediment, and *G. pulex* (representative of the biota compartment) were sampled in different campaigns over a period of 4 years (Table 1) to assess the pollution dynamics of C47, C47T1, and C47T2. Geographical coordinates and names of sampling sites are given in Supporting Information, Table S1.

Sampling and sample preparation

Grab sampling of surface water. To assess the longitudinal concentration profile of the Holtemme River, grab water samples were taken on 6 October 2015 at 18 sites along the whole river course using Lagrangian sampling (i.e., following the same water package downstream). Travel times were estimated for the actual discharge on this day and modeled discharge to travel time relationships based on time series analyses of discharge data from continuous gauging stations and distances between the sampling sites. On the sampling day, the discharge at the downstream location Nienhagen (site 38, river km 40) was only 0.340 m^3/second after a long dry period, which was below the mean lowest annual discharge of 0.406 m^3/second (period 1983–2015). In addition, eleven tributaries and the effluents of the Silstedt and Halberstadt WWTPs were sampled (Beckers et al., 2020).

Aliquots of 1 ml were transferred into 2-ml autosampler vials and stored at –20 °C. Prior to analysis, 25 µl of an internal standard mixture in methanol, containing 40 isotope-labeled compounds at 40 ng/ml, 25 µl of methanol, and 10 µl of 2 M ammonium formate buffer (pH 3.5), were added.

Large-volume solid-phase extraction sampling of surface water. Time-proportional composite water samples (28 days) were taken using an on-site large volume solid phase extraction (LVSPE) device (Schulze et al., 2017; Välitalo et al., 2017) over 3 years during March to November (Table 1). To this end, 100 l of water were extracted on-site within 14 days using a tailor-made SPE column filled with 10 g of Chromabond HR-X (Macherey-Nagel). Samples of two consecutive 14-day intervals were combined. The sampling frequency for each subsample was 100 minutes (site 17) or 60 minutes (sites 3, 38). Two of the LVSPE samplers were installed in automated measurement stations (UFZ MOBICOS) located at the Holtemme River (Fink et al., 2020) and one in a closed trailer. The sample inlets for LVSPE were located approximately 50 cm distance from and 15 to 20 cm above the streambed under base flow conditions. Details of the method are provided in Supporting Information, Section S1.2.

Sampling of WWTP influent and effluent. Twelve consecutive 2-hour composite water samples were collected from the influent and effluent of the Silstedt WWTP. The samples were collected on 9 and 10 October 2017 and 12 and 13 October 2017, respectively, accounting for the hydraulic retention time of 72 hours. Each sample was composed from subsamples taken every 2 minutes by an automatic sampler used in the routine monitoring by the WWTP operator. Samples were stored at –20 °C. For analysis, sample aliquots of 20 µl were diluted 50-fold in LC-MS-grade water, and the internal standard mixture, methanol, and buffer were added as for the surface water samples.

Gammarus pulex. *Gammarus pulex* was sampled in April 2016 according to a protocol by Hering et al. (2004) at sites 17, 36, and 38 (Table 1). Briefly, 20 samples were taken from an area of 1 m^2 at each site with a Surber sampler (500 µm mesh size). A subset of 24 specimens with different size classes was collected to avoid bias caused by different ages and stored at –20 °C. Homogenization was carried out by pulverized liquid extraction (Miller et al., 2015), and the extraction procedure followed a modified quick, easy, cheap, effective, rugged, and safe protocol according to Inostroza et al. (2016). Details of the method are given in Supporting Information, Section S1.3.

Sediment and suspended particulate matter. On 7 April 2016 approximately 300 g of superficial sediment (top 5 cm) were collected from 10 spots within an area of 5 m^2 using a stainless-steel scoop at sampling site 36, where a sedimentation zone is created by a weir. Beyond site 36 and a nearby second weir, no further sedimentation zones exist. The river bottom is characterized by large stones and pebbles. Thus, we used stainless-steel traps (Schulze et al., 2007) at sites 17 and 38 to collect suspended particulate matter (SPM) as a proxy for sediment between 9 March and 7 April 2016. Approximately 18 g of SPM were trapped at site 17 and 25 g at site 38. Samples were transported to the laboratory in cooling boxes at 4 °C. The sediment was homogenized overnight, freeze-dried, sieved to <63 µm, and stored at –20 °C.

TABLE 1: Overview of the different sampling campaigns, sampling sites, and dates as well as information on the calibration used

Sampling campaign	Sample type	Sampling date	Sites	Type of simultaneous calibration for C47 and C47T2	Type of retrospective calibration for C47T1
1	Grab water sample	6 October 2015	Holtemme River: 3, 9, 11, 13, 15, 17, 18, 21, 22, 24, 25, 26, 31, 34, 36, 38, 40, 42 Tributaries: 5, 8, 12, 14, 19, 20, 23, 29, 35, 39, 41	Matrix-matched, direct injection	Matrix-matched, direct injection
2	Composite water sample	9/10 October and 12/13 October 2017	Influent and effluent of WWTP Silstedt	Matrix-matched, direct injection	Matrix-matched, direct injection
3	LVSPE, 28-day composite	March–November 2014	3, 17, 38	Method- and matrix-matched by small-scale SPE	Method- and matrix-matched by small-scale SPE
4	LVSPE, 28-day composite	March–November 2015	3, 17, 38	Method- and matrix-matched by small-scale SPE	Method- and matrix-matched by small-scale SPE
5	LVSPE, 28-day composite	March–November 2016	3, 17, 38	Method- and matrix-matched by small-scale SPE	Method- and matrix-matched by small-scale SPE
6	Sediment/ SPM	7 April 2016	17, 36, 38	Method- and matrix-matched	Solvent calibration considering recovery; matrix effects are accounted for by IS
7	*Gammarus*	7 April 2016	17, 36, 38	Method- and matrix-matched	Solvent calibration considering recovery; matrix effects are accounted for by IS

C47 = 4-methyl-7-diethylaminocoumarin; C47T2 = 4-methyl-7-aminocoumarin; C47T1 = 4-methyl-7-ethylaminocoumarin; WWTP = wastewater-treatment plant; LVSPE = large-volume solid-phase extraction of water; IS = = internal standard; SPM = suspended particulate matter.

Total organic carbon (TOC) content was determined according to DIN 19539 (2016) by solid combustion using an LECO C-230 Carbon Analyser, and pH was measured in 0.005 M $CaCl_2$ solution using a pH electrode. Samples were extracted by pressurized liquid extraction (Dionex ASE 200), followed by clean-up steps according to Massei et al. (2018) with minor modifications (Inostroza et al., 2017). Further details of the method, TOC content, and pH of the samples are given in Supporting Information, Section S1.4 and Table S2.

LC-MS analysis

All environmental samples were analyzed for C47, C47T1, and C47T2 by LC–high-resolution MS (LC-HRMS; see section, *Chemical analysis using LC-HRMS*). Calibration and quantification were performed simultaneously with sample analysis for C47 and C47T2, whereas C47T1 was retrospectively quantified in the archived HRMS data using calibrations measured at a later time (see section, *Simultaneous and retrospective quantification*).

Concentrations of C47, C47T1, and C47T2 were analyzed by LC-MS/MS for determination of partitioning coefficients between sediment organic carbon and porewater (see section, *Prediction and experimental determination of organic–carbon partition coefficient values*) and between gammarid and water (see section, *Prediction and experimental determination of gammarid–water partitioning ratios*). Furthermore, the wastewater markers carbamazepine, diclofenac, metoprolol, and ^{1}H-benzotriazole and the sum of 4 + 5-methyl-^{1}H-benzotriazole (which could not be separated) and the groundwater marker metazachlor ESA were analyzed by LC-MS/MS in the longitudinal study (see section, *Chemical analysis using LC-MS/MS*). These data were published in Weitere et al. (2021).

Chemical analysis using LC-HRMS. An UltiMate 3000 LC system was coupled to a quadrupole-Orbitrap instrument (QExactive Plus), equipped with a heated electrospray ionization (ESI) source (all from Thermo Scientific). Details of the method are given in Supporting Information, Section S1.5.

Method detection limits (MDLs) were estimated based on replicate analyses of samples of the same concentration using spiking levels that were 5 to 10 times higher than the lowest detected concentration of the compound (US Environmental Protection Agency, 2011). The MDLs of the three coumarins in the directly injected and extracted water samples were between 2.7 and 6.2 ng/L and between 0.4 and 1.2 ng/L, respectively (Supporting Information, Table S4). The MDL ranged from 5.0 to 8.0 ng/g TOC in sediment and from 0.2 to 0.3 ng/g wet weight in *G. pulex*.

Chemical analysis using LC-MS/MS. For ESI-LC-MS/MS, a high-performance LC system (Agilent 1260 Infinity) was coupled to a tandem mass spectrometer (QTrap 6500; AB Sciex) with an ESI source, all controlled by Analyst software (Ver 1.6.2). Details of the analysis of wastewater/groundwater markers are described in Beckers et al. (2018). For details on LC and MS conditions for the analysis of C47, C47T1, and C47T2 for the determination of partitioning coefficients, see Supporting Information, Section S1.5. For calibration, mixed standards of all compounds were prepared in LC-MS-grade water at 15 levels between 1 and 50 000 ng/l. Methanol (5 vol%) was added for analysis.

Simultaneous and retrospective quantification

The compounds C47 and C47T2 could be quantified simultaneously because calibration standards were already run during the sample analysis (as part of a larger compound mixture). In contrast, C47T1 had to be quantified by retrospective analysis; that is, the samples measured up to 2 years earlier were quantified with newly measured calibration standards. To assess the performance of this approach, we compared the concentrations derived retrospectively (c_{retro}) and simultaneously (c_{sim}) for C47 and C47T2 by calculating the deviation according to Equation 1:

$$\text{Deviation (\%)} = \left| \left(\frac{c_{retro} \times 100}{c_{sim}} \right) - 100 \right| \quad (1)$$

In addition, a triplicate analysis of the calibration standards (see below) was done with an at least 4-week time span in between the measurements to calculate the variability of the retrospective quantification of C47, C47T1, and C47T2.

Bezafibrate-d4, atrazine-$^{13}C_3$, and imidacloprid-d4 were used as internal standards for C47, C47T1, and C47T2, respectively, to correct for matrix effects. Different sets of calibration standards were prepared for grab water samples, for samples collected by LVSPE, and for sediment and *G. pulex* samples, as shown in Table 1.

Based on the results of these comparisons (see section, *Performance of the retrospective calibration*), concentrations in the individual samples were calculated for C47T1 by retrospective calibration, which was corrected by the average deviation of C47 and C47T2 between the simultaneous and retrospective calibrations. Details on the calibration procedures are provided in Supporting Information, Section S1.6.

Calculation of elimination rates in the river

The elimination rates (Eli_{CD}) of the coumarin derivatives (CD) along the 13-km river stretch between the effluent of the WWTP of Silstedt and Halberstadt were calculated in relation to the persistent carbamazepine based on Kunkel and Radke (2012) by Equation 2.

$$Eli_{CD} = \left(1 - \frac{\frac{c_{CD,Site\ B}}{c_{CD,Site\ A}}}{\frac{c_{CBZ,Site\ B}}{c_{CBZ,Site\ A}}} \right) \times 100\% \quad (2)$$

The concentrations of the coumarin derivative at sites A and B are represented by $c_{CD,Site\ A}$ and $c_{CD,Site\ B}$ respectively, whereas $c_{CBZ,Site\ A}$ and $c_{CBZ,Site\ B}$ indicate the concentration of carbamazepine at these sites.

Prediction and experimental determination of organic–carbon partition coefficient values

Concentration-independent partitioning coefficients between sediment organic carbon and porewater (K_{OC}^{pred}) were predicted using OPERA (Ver 2.6; Mansouri et al., 2018). As a second approach to predict K_{OC} values, we used a polyparameter linear free-energy relationship (ppLFER) accounting for their concentration dependence, as proposed by Bronner and Goss (2011), for which we used an implementation in the UFZ Linear Solvation Energy Relationship (LSER) database (Ulrich et al., 2017). This approach uses the Freundlich isotherm to describe nonlinear sorption (Equation 3) where $K_{F,OC}$ denotes the Freundlich sorption coefficient normalized to OC, c_W is the water concentration, and n is the Freundlich exponent.

$$c_{sorbed\,OC} = K_{F,OC} \times c_W^{\,n} \quad (3)$$

Assuming a typical Freundlich exponent for sorption to organic matter of 0.8 (Endo et al., 2008; Zhu & Pignatello, 2005) and based on the reference concentration of 0.03 mmol/L to derive the ppLFER model in Bronner and Goss (2011), $K_{F,OC}$ can be expressed according to Equation 4.

$$K_{F,OC} = \frac{K_{OC}^{pred} \times 3 \times 10^{-2}}{(3 \times 10^{-2})^{0.8}} \quad (4)$$

In consequence, the concentration-dependent K_{OC}^{*} can be calculated for any water concentration applying Equation 5.

$$K_{OC}^{*} = \frac{K_{OC}^{pred} \times 3 \times 10^{-2}}{(3 \times 10^{-2})^{0.8}} \times c_W^{0.8} \times c_W^{-1} \quad (5)$$

Experimental partitioning constants K_{OC}^{exp} were derived for C47, C47T1, and C47T2 in a batch sorption experiment. To this end, sediment from the Saale River near the city of Calbe with a similar OC content (65 g/kg) and pH (6.93 in 0.005 M $CaCl_2$) and not containing any residues of C47, C47T1, and C47T2 was used. The experiments were set up for each compound individually at 5 concentration levels (0.01, 0.05, 0.2, 1, and 5 μg/l) by adding the corresponding amounts into a glass centrifuge tube with a poly(tetrafluoroethylene)-lined screw cap containing 0.5 g of sediment (<63 μm) and 10 ml of 0.005 M $CaCl_2$ solution. The sediment was previously equilibrated with the $CaCl_2$ solution for 24 hours. Samples were shaken during the whole exposure time of 168 hours on a horizontal shaker at 60 rpm at 20 ± 1 °C. Control samples without sediment were set up for all compounds. At 4, 8, 24, 72, and 168 hours of exposure, the tubes were centrifuged at 5000 *g* for 5 minutes, and aliquots of 15 or 30 μl were taken from each vial using a pipette. For analysis, aliquots were diluted appropriately in LC-MS-grade water, and 5 vol% of methanol were added.

Sediment organic matter–water concentration ratios (k_{SW}) before equilibrium for C47, C47T1, and C47T2 at sorption times of 4, 8, 24, 72, and 168 hours were derived by Equation 6 and are displayed in Supporting Information, Figure S5.

$$k_{SW} = \frac{c_S^m}{c_{fd,W}} \times f_{OC} \quad (6)$$

The sediment–water partitioning coefficients in equilibrium (K_{OC}^{exp}, i.e., for $t_s \rightarrow \infty$) were derived by fitting the exponential Equation 7 to the results.

$$k_{SW}(t_s) = K_{OC}^{exp} \times (1 - e^{-b \times t_s}) \quad (7)$$

Prediction and experimental determination of gammarid–water partitioning ratios

For the predicted partitioning coefficient between gammarid and water (K_{GW}^{pred}), the bioconcentration factor from OPERA (Mansouri et al., 2018) was used. In addition, K_{GW}^{pred} was predicted using a ppLFER approach (Geisler et al., 2012), as implemented in the UFZ LSER database (Ulrich et al., 2017), assuming only the lipid and protein fraction as relevant phases for a sorption of micropollutants. For calculations, the reported total lipid content (wet wt) of 1.34% (Ashauer et al., 2006), a phospholipid fraction of 25% of the total lipid content (Ashauer et al., 2010), and a protein content of 70% dry weight (Duman & Kar, 2015) were used.

For experimental determination of partitioning coefficients, gammarids were collected from the upper part of the Parthe River near Leipzig, Germany, which is less affected by anthropogenic activity. For each of the three compounds, two accumulation experiments were set up in different 500-ml glass beakers with exposure periods of 40 and 88 hours. Into each beaker containing 500 ml of Aachener Daphnien Medium (Klüttgen et al., 1994), six gammarids and one beech leaf were placed, and the compounds were dosed to a final concentration of 2 µg/l by adding 200 µl of a 5-µg/ml stock solution in methanol. The exposure was done in 500 ml at 15 °C with a 16:8-hour light:dark cycle. The water was aerated with a flow rate of approximately 1 l/minute using Pasteur pipettes connected via silicone tubing to peristaltic pumps.

Water samples were taken after 1, 40, and 88 hours to control the exposure concentrations. The exposed gammarids were sampled after 40 and 88 hours, respectively; dried carefully with tissue; transferred into centrifuge tubes for extraction; and frozen. Extraction was done as described in the section *Grammarus pulex*.

Gammarid–water concentration ratios (k_{GW}^{exp}) based on experimentally measured concentrations were calculated applying Equation 9, where c_G^m denotes the measured coumarin concentrations in gammarids (whole organism) and $c_{fd,W}^{exp}$ the experimentally derived freely dissolved water concentrations.

$$k_{GW}^{exp} = \frac{c_G^m}{c_{fd,w}^{exp}} \quad (8)$$

Calculation of freely dissolved concentrations based on experimentally derived partitioning coefficients

To understand the distribution among the compartments water, *G. pulex*, and sediments and to identify sources and sinks in the river system, equilibrium partitioning was used as a model. Chemical activities as driving forces of partitioning were determined as freely dissolved concentrations in all three matrices.

Freely dissolved water concentrations. To calculate the freely dissolved water concentrations ($c_{fd,W}^{exp}$) from the measured water concentrations (c_W^m), we used Equation 9, assuming that the partitioning coefficients between dissolved organic carbon (DOC) and water are the same as the experimentally derived, concentration-dependent partitioning coefficient between sediment organic carbon and water (K_{OC}^{exp}). To determine K_{OC}^{exp}, the freely dissolved sediment concentrations were calculated for all measured water concentrations using the linearized Freundlich equation (Supporting Information, Figure S6).

$$c_{fd,W}^{exp} = \frac{c_W^m}{1 + (f_{DOC} \times K_{OC}^{exp})} \quad (9)$$

In Equation 9, f_{DOC} is the fraction of dissolved organic matter (DOC), which was derived from measured DOC concentrations.

Freely dissolved concentrations in sediment. The freely dissolved concentration in sediment ($c_{fd,S}$) was derived by applying Equation 10, where c_S^m is the measured sediment concentration, f_{oc} is the organic carbon fraction in sediment, and K_{OC}^{exp} is the experimental partitioning coefficient between the sediment organic carbon and porewater, considering the concentration dependence of the K_{OC}.

$$c_{fd,S} = \frac{c_S^m}{f_{OC} \times K_{OC}^{exp}} \quad (10)$$

Freely dissolved concentrations in gammarid. For the calculation of freely dissolved concentrations in gammarids ($c_{fd,G}^{exp}$) on the basis of k_{GW}^{exp} by Equation 11, the average partitioning coefficient derived after 40 and 88 hours was applied.

$$c_{fd,G}^{exp} = \frac{c_G^m}{K_{GW}^{exp}} \quad (11)$$

We are aware that this is a simplification for *Gammarus* as a living organism that may actively reduce internal concentrations by metabolism and excretion until a steady-state concentration is achieved, which may be below thermodynamic equilibrium concentration.

RESULTS AND DISCUSSION

Performance of the retrospective calibration

The deviation of the retrospective from the simultaneous quantification was compared for C47 and C47T2 for the different sets of samples investigated because these compounds were quantified both simultaneously and retrospectively. The results are shown as an overview in Supporting Information, Figure S1. Compared to the simultaneous quantification, the retrospective one led to an overestimation of the concentrations of on average 11 (C47) and 17% (C47T2) in non-concentrated grab water samples, 29 (C47) and 45% (C47T2) in time-integrated samples (LVSPE-processed water samples), and 12 (C47) and 16% (C47T2) in *G. pulex*, whereas the concentrations in sediment were retrospectively underestimated by approximately 31 (C47) and 80% (C47T2). To receive a consistent data set for all three coumarin derivatives, the average deviation

between the retrospectively and simultaneously quantified C47 and C47T2 was considered in all sample types to correct the results of C47T1, which was solely retrospectively quantified using archived HRMS data.

The differences between retrospective and simultaneous calibration showed that the performance of the instrumental analysis changes over time. This is not surprising because LC columns deteriorate with prolonged use, resulting in a stronger peak tailing and loss of separation power. In addition, contamination of the MS with sample residues results in decreasing sensitivity. While a regular cleaning of the ion source and rinsing of the column were performed, a more intense cleaning of the ion lens system and a change of the LC column were done only at specific intervals. Thus, for a retrospective calibration conducted up to 3 years after analysis of samples, the instrument performance state is randomly different from the one during the simultaneous calibration, which results in a variability of up to 18% (Supporting Information, Table S6), as indicated by the triplicate injection of the same calibration standards with at least a 4-week time span in between.

Overall, the results suggest that within a typical error margin of approximately 20 to 30% a retrospective quantification of compounds from LC-HRMS screening data is possible. To obtain a more consistent data set, we calculated concentrations of C47 and C47T2 using simultaneous calibration and concentrations of C47T1 using retrospective calibration, which was corrected by the average deviation of C47 and C47T2 between the simultaneous and retrospective calibrations for the four sample types.

Longitudinal concentration profile

We detected C47 and its two derivatives along the whole Holtemme River stretch between WWTP Silstedt and the confluence with the Bode River 42 km farther downstream (Figure 3). We measured the highest concentrations for C47 (0.50 µg/l), C47T1 (0.75 µg/l), and C47T2 (1.25 µg/l) close to the effluent of WWTP Silstedt at site 17. Thus, WWTP Silstedt was clearly confirmed as the source of discharge into the river. Also, the wastewater marker compounds carbamazepine, diclofenac, metoprolol, ^{1}H-benzotriazole, and 4+5-methyl-^{1}H-benzotriazole, which where quantified to disentangle the process influencing the fate of the coumarin derivatives, were discharged by WWTP Silstedt. None of the coumarin derivatives was detected in the effluent of WWTP Halberstadt (site 29). Consequently, other than for the 5 general wastewater markers, no additional increase in the concentration of the coumarin derivatives was observed.

In seven tributaries, also none of the coumarin derivatives could be detected, whereas in some the presence of the two benzotriazoles, metoprolol, diclofenac, and carbamazepine indicated an input of municipal wastewater (Supporting Information, Figure S2). The two tributaries farthest downstream (sites 39 and 41) contained coumarin derivative levels similar to those of the Holtemme River along with the five wastewater markers. These tributaries are connected upstream to the Holtemme River, and thus, the water sampled there originated probably to a large extent from the Holtemme River itself.

The concentrations of C47, C47T1, and C47T2 decreased by approximately 53% from site 17 to site 26 and further to approximately 16% to site 42. To understand the underlying processes, we compared the longitudinal profiles of the coumarins with those of well-known wastewater markers simultaneously emitted from the WWTPs and the groundwater marker metazachlor ESA. To this end, we plotted the relative concentrations along each river stretch downstream of the two WWTPs (i.e., sites 17–26 and 31-42, respectively) against the travel times, as shown in Supporting Information, Figure S3. While diclofenac and metoprolol showed a continuous decrease with travel time, this decrease was visible, but less prominent, for the coumarins carbamazepine and both benzotriazoles, which showed a rather similar pattern.

The concentration decrease of diclofenac can be considered as a proxy for photodegradation in river systems, as suggested by Schmitt et al. (2021). These authors also suggested that metoprolol is affected not by photodegradation but by biodegradation in rivers. The decrease of both compounds being stronger than that of the coumarins indicates that coumarins are less susceptible to photodegradation and biodegradation, respectively, than these compounds and are similarly persistent as carbamazepine or the benzotriazoles.

As a more detailed approach, we calculated elimination rates relative to the rather persistent carbamazepine for this river stretch according to Equation 2 based on Kunkel and Radke (2012). Thus, C47, C47T1, and C47T2 concentrations were normalized to that of carbamazepine to compensate for dilution (Supporting Information, Table S7). Normalized values >0 indicate attenuation by transformation (Kunkel & Radke, 2012), sorption to sediment, SPM, biofilms, and other biota (Kunkel & Radke, 2011; Radke et al., 2010). This approach assumes that carbamazepine is not degraded over the respective river section, which might not always be the case. For instance, Writer et al. (2013) reported a degradation half-life of 21 hours in a river. However, the traveling times in the present study were comparably shorter, approximately 3.4 hours between sites 17 and 26 and approximately 6.1 hours between sites 31 and 42.

Low relative elimination rates between the site 17 (downstream of WWTP Silstedt) and site 26 (upstream of WWTP Halberstadt) of C47 (8%), C47T1 (16%), and C47T2 (22%) indicated dilution as the main cause of the strong concentration decrease. Along this stretch, the concentration of metazachlor ESA increased from 34 ng/l at site 17 to 59 ng/l at site 26, suggesting that the diluting water contained substantial concentrations of this compound. Because it was not detected in any of the tributaries contributing in this river stretch and ESA transformation products of chloroacetanilide herbicides are well-known groundwater contaminants in agricultural areas (Huntscha et al., 2008), this suggests that an inflow of groundwater is the main cause of this dilution.

In contrast, the concentration profiles of the three coumarins downstream of WWTP Halberstadt indicated higher elimination

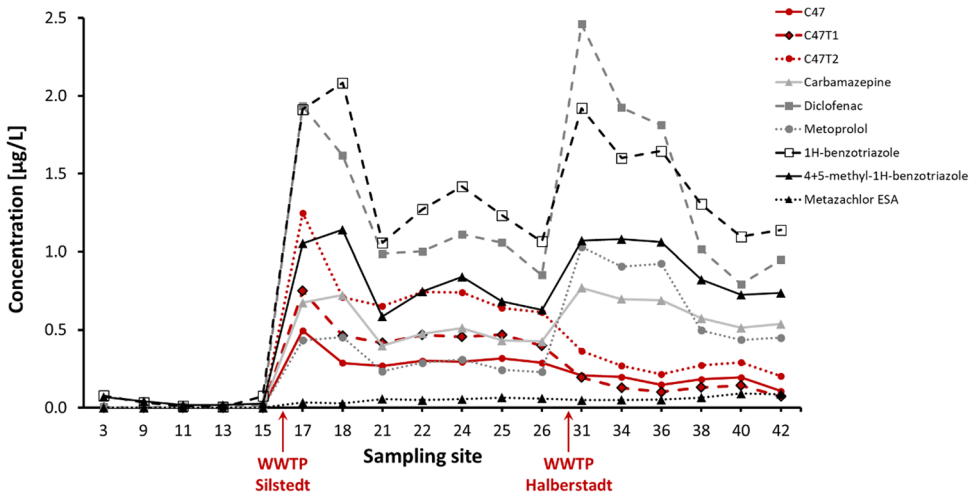

FIGURE 3: Concentration profiles of C47, C47T1, and C47T2; the wastewater tracers carbamazepine, diclofenac, metoprolol, 4+5-methylbenzotriazole, and benzotriazole; as well as the groundwater marker metazachlor ethane sulfonic acid in the longitudinal profile of the Holtemme on 6 October 2015. C47 = 4-methyl-7-diethylaminocoumarin; C47T1 = 4-methyl-7-ethylaminocoumarin; C47T2 = 4-methyl-7-aminocoumarin; ESA = ethane sulfonic acid; WWTP = wastewater-treatment plant.

rates between sites 31 and 42 of C47 (26%), C47T1 (46%), and C47T2 (19%) along with longer travel times, thus suggesting that the attenuation, especially of C47T1 in this river stretch, is not solely based on dilution (Supporting Information, Table S7). In general, our results suggest only a limited elimination of C47 and its derivatives due to photo- or biotransformation or sorption in the Holtemme River. However, the present longitudinal study was conducted on a cloudy day in October; thus, photolysis and biotransformation might be higher during the summer months with higher temperatures and irradiation.

Transformation of C47 to C47T1 and C47T2 in WWTP Silstedt

The well-known transformation of secondary and tertiary amines by *N*-dealkylation in activated sludge (Gulde et al., 2016) raised the hypothesis that C47T1 and C47T2 are originating from transformation of C47 within WWTP Silstedt. To this end, the WWTP influent was sampled on 9 October 2017 in 2-hour intervals and the corresponding effluent on 12 October 2017. This time difference accounts for the hydraulic retention time of the WWTP of approximately 72 hours (Figure 4).

The fluctuation of coumarin concentrations in the 2-hour influent samples was leveled out to a large extent in the effluent because it could be expected for a well-mixed WWTP system with a large hydraulic retention time. The suspected biotransformation of C47 is confirmed by the decrease of the average concentration from 3.0 to 1.6 µg/l during the WWTP passage treatment and the simultaneously occurring concentration increase of C47T1 (from 0.1 to 0.9 µg/l) and C47T2 (from 0.2 to 0.5 µg/l). Applying a molar concentration balance approach of the average concentrations on 9 October 2017 shows that the transformed amount of C47 (66 of 138 mmol/l in the influent) can be explained by the formed amounts of C47T1 (42 mmol/l) and C47T2 (20 mmol/l), thus confirming the assumed degradation of C47 to C47T1 and C47T2. Formation of the *N*-oxide, which is also a common biotransformation pathway for tertiary amines (Gulde et al., 2016), was not evident because we could not detect a peak for the exact mass of this compound ($C_{14}H_{17}NO_3$+H^+, *m/z* 248.1281) in the LC-HRMS data.

In consequence, the WWTP of Silstedt was continuously discharging the 3 endocrine active coumarin derivatives in the grams per day range into the Holtemme River.

Seasonal variation in LVSPE samples

The temporal concentration variations were assessed from 28-day composite samples ($n = 96$) that were collected in spring, summer, and autumn from 2014 to 2016 using an LVSPE upstream of Wernigerode (site 3), downstream of WWTP Silstedt (site 17), and at Nienhagen (site 38). In winter, sampling was not possible because the monitoring stations were not equipped for sampling at low temperatures. Within these 3 years none of the coumarin derivatives was detected at site 3 (Wernigerode). However, all three coumarins were quantified in sites 17 and 38, with the highest concentrations downstream of WWTP Silstedt (site 17; Figure 5). The high concentrations of the coumarin derivatives at site 17 across our sampling campaigns suggest a continuous emission from WWTP Silstedt. Concentrations at site 17 varied within a factor of 5 to 10 for each compound within each year. Average concentrations were in the same order of magnitude observed in the longitudinal profile (Figure 3) on 6 October 2015 (1.6 vs. 0.5 µg/l for C47, 0.7 vs. 0.7 µg/l for C47T1, and 0.7 vs. 1.2 µg/l for C47T2). For C47, no clear trend within the concentration profiles between the seasons or the 3 years was observed. In contrast, the concentration ratios of the three compounds, especially

that of C47 to C47T2, showed a large variation; for example, in 2015 it varied between 0.8 and 36.9 at site 17 (Supporting Information, Figure S4). By far the highest C47 to C47T1/C47T2 ratios in all three consecutive years were observed in spring and the lowest ratios in late summer. These variations might be caused by an input of mixtures of varying composition of the three coumarins into the WWTP or a higher microbial transformation of C47 to C47T1 and C47T2 in the summer months at higher temperatures. The ratios of C47T1 and C47T2 to C47 were for most sampling periods similar at sites 17 and 38, whereas concentrations were typically 3 to 5 times lower. However, peak concentrations observed at site 38 were less prominent than at site 17, especially for the transformation products in summer 2016, which suggests that both dilution and degradation contribute to this concentration decrease in the Holtemme River.

Comparison of predicted and experimental partitioning coefficients

Partitioning between sediment and water. Concentration ratios (k_{SW}) between sediment organic carbon and water at initial water concentrations of the three coumarin derivatives of 0.2, 1, and 5 µg/l were estimated after exposure for up to 168 hours in a batch sorption experiment by Equation 6. At initial water concentrations of 0.01 and 0.05 µg/l, the compounds could not be detected. The k_{SW} values showed a strong increase within the first 72 hours of sorption time to sediment, whereas the increase was much smaller up to 168 hours, suggesting that the system was close to equilibrium after 168 hours (Supporting Information, Figure S5). We did not detect C47T1 or C47T2 in the sorption experiment of C47 or C47T2 in the sorption experiment of C47T1. Thus, microbial degradation of the compounds in the course of the sorption experiment likely did not occur. Partitioning coefficients between sediment organic matter and water in equilibrium (K_{OC}^{exp}) were derived from fitted k_{SW} values applying Equation 7 (see Supporting Information, Table S8). The K_{OC}^{exp} values were higher for lower initial concentrations of all three compounds, indicating a strong concentration dependence of sorption that may be caused by sorption sites with different affinity for cation exchange, as reported in the literature for other aromatic amines (Li et al., 2001; Richter et al., 2009). Thus, we did not use a single K_{OC}^{exp} value for each compound to determine freely dissolved concentrations in the sediment porewater but calculated these from nonlinear sorption isotherms based on the measured sediment concentrations. These nonlinear isotherms were approximated using the Freundlich equation, which showed a good fit of the data (Supporting Information, Figure S6).

A comparison of experimental and predicted K_{OC} values (concentration-dependent by ppLFER and constant using

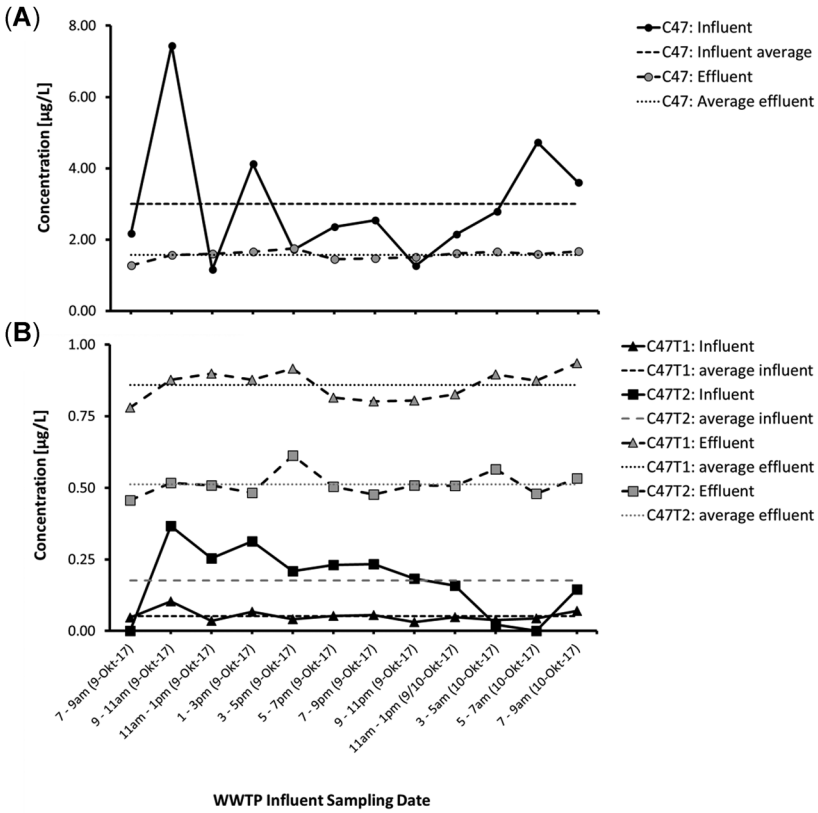

FIGURE 4: Concentration profiles of (**A**) C47 and (**B**) C47T1 and C47T2 in the influent (continuous line) and the effluent (dashed line) of the wastewater-treatment plant (WWTP) Silstedt in March 2017. Effluent was sampled 72 hours after the influent to account for the hydraulic retention time of the WWTP. C47 = 4-methyl-7-diethylaminocoumarin; C47T1 = 4-methyl-7-ethylaminocoumarin; C47T2 = 4-methyl-7-aminocoumarin.

OPERA) is shown in Figure 6 for C47 and in Supporting Information, Figure S7 for C47T1 and C47T2.

With both prediction tools, derived K_{OC} values were in the same range and were up to 2.6-fold higher for C47 when using ppLFER compared to OPERA. Values for C47T1 and C47T2 were up to 11.6 and 13.3 times lower, respectively, when calculated with ppLFER compared to OPERA. However, the predicted K_{OC} values were up to 33-fold (C47), 54-fold (C47T1), and 93-fold (C47T2) lower than the concentration-dependent K_{OC} values derived by the batch sorption experiment. This indicates that strong sorption mechanisms might contribute to the partitioning, which are not explicitly covered in both K_{OC} prediction models based on structure. A possible explanation is cation exchange based on Coulomb interactions, which are by far the most potent intermolecular forces. Their influence on the partitioning of sulfonamides to organic matter even at pH values greater than the dissociation constant (pK_a) + 3 (Richter et al., 2009) or on the sorption of other aromatic amines to soil even at pH values >pK_a + 2 (Li et al., 2001) has been demonstrated. Because we could not find any experimental pK_a values for the coumarins, these were predicted using the OPERA and JChem software. Using JChem Calculator Plugins, basic pK_a values of 4.3 for C47 and C47T1 and 3.4 for C47T2 were predicted, whereas those calculated by OPERA were approximately 2 orders of magnitude higher (6.7 for C47, 6.6. for C47T1, and 5.6 for C47T2). Despite these huge uncertainties, pK_a values in this order of magnitude suggest cation exchange as a plausible cause of the strong sorption at sediment pH values of approximately 6.8.

Thus, experimental data are likely superior to evaluate the partitioning of ionizable compounds between water and sediment compared to predictions using ppLFER. Furthermore, biased predictions may be also attributed to the presence of strongly adsorbing black carbon in the sediment (Burkhard et al., 2008). In consequence, the following

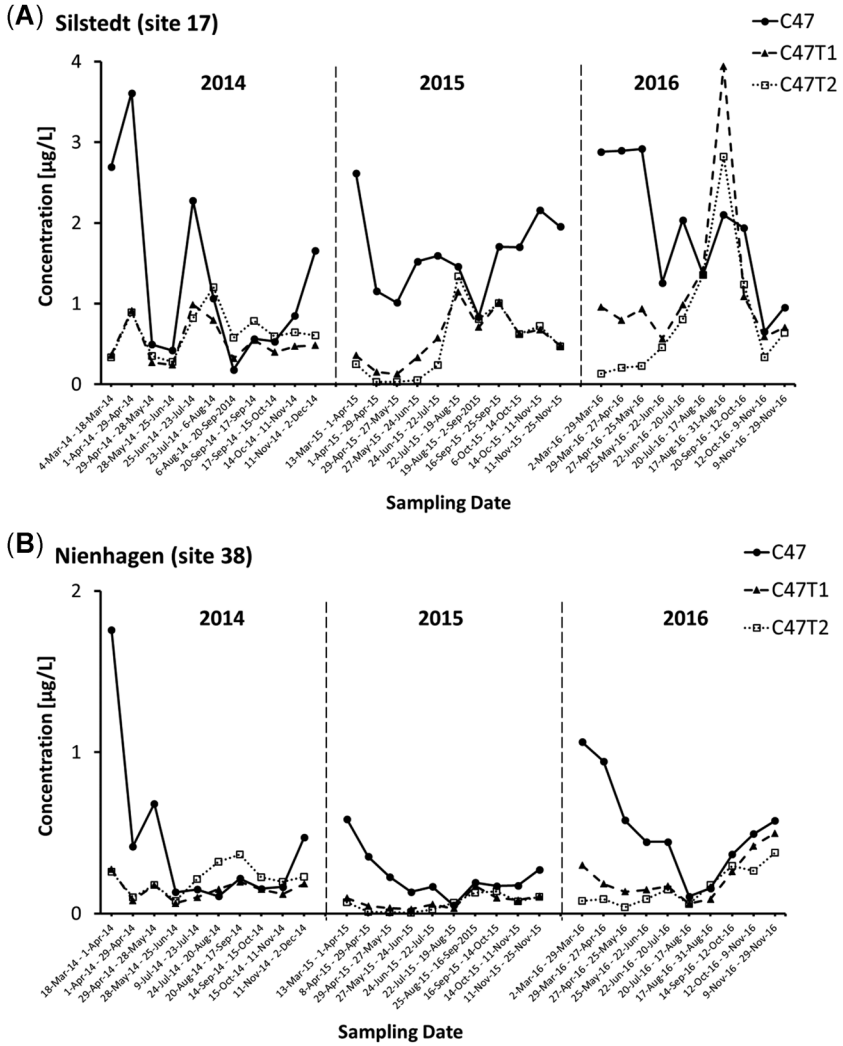

FIGURE 5: Temporal concentration profile in 28-day composite large-volume solid-phase extraction samples of C47, C47T1, and C47T2 collected at (**A**) Silstedt and (**B**) Nienhagen (note the different scale) between 2014 and 2016. C47 = 4-methyl-7-diethylaminocoumarin; C47T1 = 4-methyl-7-ethylaminocoumarin; C47T2 = 4-methyl-7-aminocoumarin.

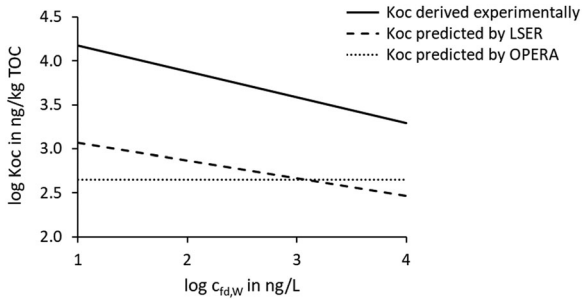

FIGURE 6: Overview of partitioning coefficients of 4-methyl-7-diethylaminocoumarin between sediment organic carbon and pore-water derived by experimental evaluation and predicted constant as well as concentration-dependent values derived with OPERA (Mansouri et al., 2018) and the polyparameter linear free-energy relationship (Ulrich et al., 2017). K_{OC} = organic–carbon partition coefficient; TOC = total organic carbon; LSER = Linear Solvation Energy Relationship (database).

discussion (see *Water–sediment partitioning and uptake into* G. pulex *in the river*) is based on experimentally derived K_{OC} values.

Partitioning between gammarid and water. Experimentally derived steady-state bioaccumulation factors from the gammarid uptake experiment with OPERA and ppLFER predicted that partitioning coefficients (K_{GW}) between gammarid and water solely deviate by factors of 1.4 and 2.1 (C47), 1.5 and 1.0 (C47T1), and 5.1 and 0.8 (C47T2), respectively, as shown in Supporting Information, Table S9. Thus, the application of ppLFER results in a better fit of experimental and predicted values with an average deviation of factor 1.3 versus 2.7 for OPERA. However, for a rough estimate, equilibrium partitioning seems to be an appropriate model for the prediction of concentrations of these compounds in *G. pulex*, also supporting hydrophobic interactions as the driving force of partitioning. Hence, the body burden of *G. pulex* can be estimated from water concentrations of the coumarins by applying equilibrium partitioning theory (EqP; Di Toro et al., 1991). However, the observed deviations from the model indicate that metabolization might be not negligible.

Water/sediment partitioning and uptake into G. pulex in the river

To understand the fate of the coumarins in the Holtemme River, the distribution between water, sediment (or SPM), and biota (*G. pulex*) was analyzed using EqP. In a first step, we assessed to what extent a binding of the coumarins to dissolved organic matter in the water phase might play a role or whether there are only minor deviations between the measured and freely dissolved water concentrations.

To this end, we used Equation 9 with the experimental K_{OC} values determined previously and the DOC concentration in the Holtemme River between 3.5 and 4.8 mg/l (as available from the State Office for Flood Protection and Water Management Saxony-Anhalt, 2019). Our results showed that for all sites and compounds no more than 2% of the measured water concentration is likely bound to dissolved organic matter (Supporting Information, Table S10).

Freely dissolved concentrations of the coumarins in sediments/SPM and gammarids were estimated according to Equations 10 and 11 for the sites downstream of WWTP Silstedt (site 17), Gross Quenstedt (site 36), and Nienhagen (site 38). Ratios of freely dissolved concentrations in a range

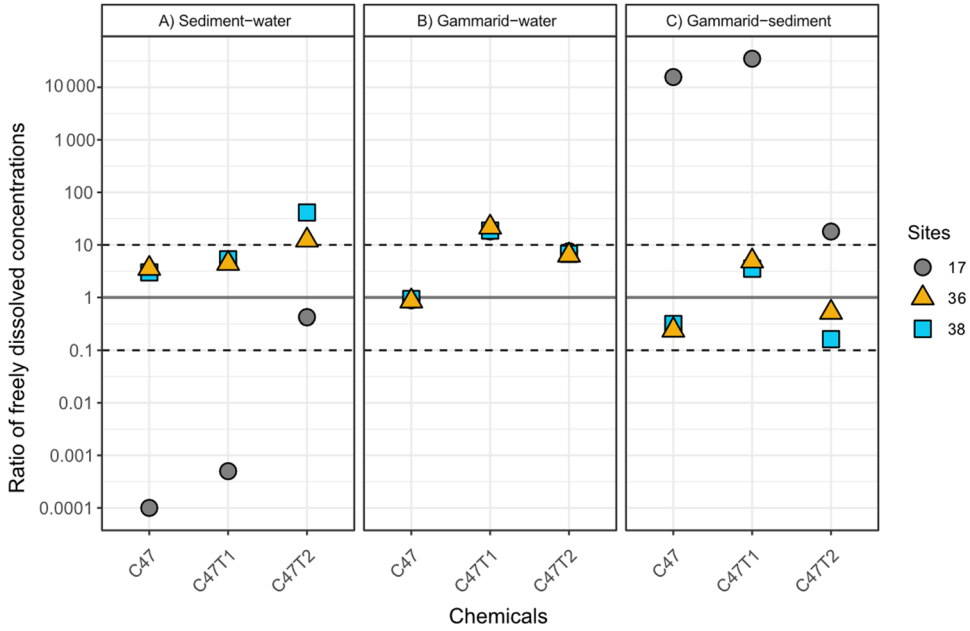

FIGURE 7: Ratio of calculated freely dissolved concentrations in gammarid tissues, water, and sediment for C47, C47T1, and C47T2 in the Holtemme River. Ratios were calculated for sites 17, 36, and 38 on the basis of experimentally derived partitioning coefficients. A state close to equilibrium partitioning is considered in the range of $0.1 \leq \text{ratio} \leq 10$. C47 = 4-methyl-7-diethylaminocoumarin; C47T1 = 4-methyl-7-ethylaminocoumarin; C47T2 = 4-methyl-7-aminocoumarin.

from 0.1 to 10 are assumed to reflect conditions close to equilibrium of partitioning (or steady state) between the corresponding compartments (Inostroza et al., 2017). We are aware that a dynamic river system will never be at a true equilibrium state; nevertheless, this type of data evaluation provides valuable hints at potential sources and sinks among the different compartments in a river.

The concentrations determined by LVSPE from 29 March to 27 April 2016 were used for these calculations. No LVSPE samples were available for site 36; thus, the concentration from the nearby site 38 was used because in the stretch between these two sites no significant tributaries are located.

Experimentally derived partitioning coefficients of the three coumarin derivatives between water, sediment, and biota were applied to evaluate their fate in the Holtemme River (Figure 7). The partitioning of the coumarins between sediment and water is close to equilibrium in the sedimentation zone at site 36 and at site 38 (Figure 7A). In contrast, ratios of the freely dissolved concentrations of 6×10^{-5} (C47), 5×10^{-4} (C47T1), and 0.4 (C47T2) indicate conditions far from equilibrium for C47 and C47T1 between sediment and water close to WWTP Silstedt at site 17. This suggests that the contact time of the coumarins with the trapped SPM is not sufficient to reach an approximate equilibrium because these compounds are emitted from the WWTP in dissolved form, while the SPM is transported to this site from upstream. For C47T1 and C47T2, a trend toward high ratios of freely dissolved concentrations between sediment and water up to 42.5 (Supporting Information, Table S10) is most likely caused by *N*-dealkylation of C47 within the sediment porewater, resulting in increasing concentrations of its transformation products.

At the field sites, all coumarin derivatives were closer to equilibrium for the partitioning between gammarids and water (Figure 7B). Based on experimentally derived steady-state accumulation factors taken as estimates for equilibrium partition coefficients, the average ratio of the freely dissolved concentration of C47 between gammarid and water is slightly <1 (0.9), suggesting a close to equilibrium situation. The derivatives C47T1 and C47T2 are accumulated on average by approximately 1 order of magnitude more (factors 19.8 and 7.1, respectively) in field-sampled *G. pulex* than predicted from laboratory bioaccumulation experiments. This may be caused by the presence of C47 in the field-sampled organisms and its partial metabolization to C47T1 and C47T2 and limited excretion of the latter that might result in above-equilibrium concentrations. This interpretation is underlined by the detection of C47T1 and C47T2 in *G. pulex* that were solely exposed to C47 in the uptake experiment.

The partitioning of the coumarins between gammarid and sediment reflects the combinations of sediment and water and of *Gammarus* and water partitioning and shows major deviations from equilibrium close to their point source at site 17 (Figure 7C).

CONCLUSIONS

The WWTP of Silstedt was confirmed as a source that is continuously discharging the antiandrogens C47, C47T1, and C47T2 in the grams per day range into the Holtemme River. This results in exposure concentrations in water in the low micrograms per liter range at all sites downstream of the WWTP. The attenuation of coumarins in the river is mainly caused by dilution, while transformation was of minor importance. At WWTP Silstedt, *N*-dealkylation of C47 to the less potent but still antiandrogenic substances C47T1 and C47T2 occurred, but the data indicate a high persistence of C47 in wastewater treatment. Predicted partitioning coefficients between gammarids and water were in good agreement with measured steady-state bioaccumulation, suggesting hydrophobic interactions as the driving force of partitioning. Deviations between experimental steady-state bioaccumulation factors and field observations indicate that C47T1 and C47T2 might accumulate in organisms in concentrations above thermodynamic equilibrium as a result of continuous supply from C47 transformation. The exceedance of predicted hydrophobicity-based partition coefficients by experimentally derived partition coefficients between water and sediment by approximately 2 orders of magnitude suggests that a small set of sorption experiments as done in the present study might be more appropriate than relying on partitioning predictions that are not able to consider ionic interactions.

Supporting Information—The Supporting Information is available on the Wiley Online Library at https://doi.org/10.1002/etc.5181.

Acknowledgment—The present study was supported by the European FP7 Collaborative Project SOLUTIONS (grant 603437). We thank the WWTP Silstedt operator for providing influent and effluent samples. A. Musolff (UFZ) is acknowledged for calculating flow velocities/travel times of the river. We thank J. Ahlheim, M. Petre, A. Piotrowska, and H. Schupke (all UFZ) for their substantial support of sampling and laboratory work and V. Svara (UFZ) for his advice on setting up the *Gammarus* exposure experiment. A free academic license of JChem for Office (Excel) and the JChem Calculator Plugins was used for structure-based property calculations, which we gratefully acknowledge (JChem for Office 6.2.1,2014, ChemAxon). The QExactive Plus LC-HRMS used is part of the major infrastructure initiative CITEPro (Chemicals in the Terrestrial Environment Profiler) funded by the Helmholtz Association. MOBICOS was funded as a large investment by the German Federal Ministry of Education and Research under the Programme Oriented Funding at the Helmholtz Centre for Environmental Research–UFZ. L.-M. Beckers' present address is Department of Aquatic Chemistry, Federal Institute of Hydrology, Koblenz, Germany.

Author Contributions Statement—M. Muschket and M. Krauss: writing–manuscript. W. Brack: supervision and editorial assistance. P. A. Inostroza: evaluation of partitioning data; L.-M. Beckers: performance of experiments. T. Schulze: provision of LVSPE samples.

Data Availability Statement—Data, associated metadata, and calculation tools are available from the corresponding author

(matthias.muschket@ufz.de). All MS data (>100 GB) are permanently stored on the server of the institute (Helmholz Centre for Environmental Research) and can also be provided by the corresponding author.

REFERENCES

Ashauer, R., Boxall, A., & Brown, C. (2006). Uptake and elimination of chlorpyrifos and pentachlorophenol into the freshwater amphipod *Gammarus pulex*. *Archives of Environmental Contamination and Toxicology*, *51*, 542–548.

Ashauer, R., Caravatti, I., Hintermeister, A., & Escher, B. I. (2010). Bioaccumulation kinetics of organic xenobiotic pollutants in the freshwater invertebrate *Gammarus pulex* modeled with prediction intervals. *Environmental Toxicology and Chemistry*, *29*, 1625–1636.

Beckers, L. M., Brack, W., Dann, J. P., Krauss, M., Müller, E., & Schulze, T. (2020). Unraveling longitudinal pollution patterns of organic micropollutants in a river by non-target screening and cluster analysis. *Science of the Total Environment*, *727*, Article 138388.

Beckers, L. M., Busch, W., Krauss, M., Schulze, T., & Brack, W. (2018). Characterization and risk assessment of seasonal and weather dynamics in organic pollutant mixtures from discharge of a separate sewer system. *Water Research*, *135*, 122–133.

Bronner, G., & Goss, K. U. (2011). Predicting sorption of pesticides and other multifunctional organic chemicals to soil organic carbon. *Environmental Science & Technology*, *45*, 1313–1319.

Burkhard, L. P., Cook, P. M., & Lukasewycz, M. T. (2008). Organic carbon–water concentration quotients (Πsocs and πpocs): Measuring apparent chemical disequilibria and exploring the impact of black carbon in Lake Michigan. *Environmental Science & Technology*, *42*, 3615–3621.

Di Paolo, C., Kirchner, K., Balk, F. G. P., Muschket, M., Brack, W., Hollert, H., & Seiler, T. B. (2016). Downscaling procedures reduce chemical use in androgen receptor reporter gene assay. *Science of the Total Environment*, *571*, 826–833.

Di Toro, D. M., Zarba, C. S., Hansen, D. J., Berry, W. J., Swartz, R. C., Cowan, C. E., Pavlou, S. P., Allen, H. E., Thomas, N. A., & Paquin, P. R. (1991). Technical basis for establishing sediment quality criteria for nonionic organic chemicals using equilibrium partitioning. *Environmental Toxicology and Chemistry*, *10*, 1541–1583.

DIN 19539. (2016). Untersuchung von Feststoffen – Temperaturabhängige Differenzierung des Gesamtkohlenstoffs (TOC400, ROC, TIC900). *Deutsches Institut für Normung*.

Duman, F., & Kar, M. (2015). Evaluation of effects of exposure conditions on the biological responses of *Gammarus pulex* exposed to cadmium. *International Journal of Environmental Science and Technology*, *12*, 437–444.

Endo, S., Grathwohl, P., Haderlein, S. B., & Schmidt, T. C. (2008). Compound-specific factors influencing sorption nonlinearity in natural organic matter. *Environmental Science & Technology*, *42*, 5897–5903.

European Chemicals Agency. (2020). 7-(Diethylamino)-4-methyl-2-benzopyrone. Helsinki, Finland. Retrieved June 30, 2021, from https://echa.europa.eu/de/registration-dossier/-/registered-dossier/18846/1

Fink, P., Norf, H., Anlanger, C., Brauns, M., Kamjunke, N., Risse-Buhl, U., Schmitt-Jansen, M., Weitere, M., & Borchardt, D. (2020). Streamside mobile mesocosms (MOBICOS): A new modular research infrastructure for hydro-ecological process studies across catchment-scale gradients. *International Review of Hydrobiology*, *105*, 63–73.

Geisler, A., Endo, S., & Goss, K. U. (2012). Partitioning of organic chemicals to storage lipids: Elucidating the dependence on fatty acid composition and temperature. *Environmental Science & Technology*, *46*, 9519–9524.

Gulde, R., Meier, U., Schymanski, E. L., Kohler, H. P. E., Helbling, D. E., Derrer, S., Rentsch, D., & Fenner, K. (2016). Systematic exploration of biotransformation reactions of amine-containing micropollutants in activated sludge. *Environmental Science & Technology*, *50*, 2908–2920.

Hering, D., Moog, O., Sandin, L., & Verdonschot, P. F. M. (2004). Overview and application of the AQEM assessment system. *Hydrobiologia*, *516*, 1–20.

Huntscha, S., Singer, H., Canonica, S., Schwarzenbach, R. P., & Fenner, K. (2008). Input dynamics and fate in surface water of the herbicide metolachlor and of its highly mobile transformation product metolachlor ESA. *Environmental Science & Technology*, *42*, 5507–5513.

Inostroza, P. A., Massei, R., Wild, R., Krauss, M., & Brack, W. (2017). Chemical activity and distribution of emerging pollutants: Insights from a multi-compartment analysis of a freshwater system. *Environmental Pollution*, *231*, 339–347.

Inostroza, P. A., Wicht, A. J., Huber, T., Nagy, C., Brack, W., & Krauss, M. (2016). Body burden of pesticides and wastewater-derived pollutants on freshwater invertebrates: Method development and application in the Danube River. *Environmental Pollution*, *214*, 77–85.

Kitamura, N., Fukagawa, T., Kohtani, S., Kitoh, S. I., Kunimoto, K. K., & Nakagaki, R. (2007). Synthesis, absorption, and fluorescence properties and crystal structures of 7-aminocoumarin derivatives. *Journal of Photochemistry and Photobiology, A: Chemistry*, *188*(2), 378–386.

Klüttgen, B., Dülmer, U., Engels, M., & Ratte, H. T. (1994). ADaM, an artificial freshwater for the culture of zooplankton. *Water Research*, *28*, 743–746.

Krauss, M., Hug, C., Bloch, R., Schulze, T., & Brack, W. (2019). Prioritising site-specific micropollutants in surface water from LC-HRMS non-target screening data using a rarity score. *Environmental Sciences Europe*, *31*, Article 45.

Kunkel, U., & Radke, M. (2011). Reactive tracer test to evaluate the fate of pharmaceuticals in rivers. *Environmental Science & Technology*, *45*, 6296–6302.

Kunkel, U., & Radke, M. (2012). Fate of pharmaceuticals in rivers: Deriving a benchmark dataset at favorable attenuation conditions. *Water Research*, *46*, 5551–5565.

Lacy, A., & O'Kennedy, R. (2004). Studies on coumarins and coumarin-related compounds to determine their therapeutic role in the treatment of cancer. *Current Pharmaceutical Design*, *10*, 3797–3811.

Li, H., Lee, L. S., Fabrega, J. R., & Jafvert, C. T. (2001). Role of pH in partitioning and cation exchange of aromatic amines on water-saturated soils. *Chemosphere*, *44*, 627–635.

Loos, R., Hanke, G., & Eisenreich, S. J. (2003). Multi-component analysis of polar water pollutants using sequential solid-phase extraction followed by LC-ESI-MS. *Journal of Environmental Monitoring*, *5*, 384–394.

Mansouri, K., Grulke, C. M., Judson, R. S., & Williams, A. J. (2018). OPERA models for predicting physicochemical properties and environmental fate endpoints. *Journal of Cheminformatics*, *10*, Article 10.

Massei, R., Byers, H., Beckers, L. M., Prothmann, J., Brack, W., Schulze, T., & Krauss, M. (2018). A sediment extraction and cleanup method for wide-scope multitarget screening by liquid chromatography–high-resolution mass spectrometry. *Analytical and Bioanalytical Chemistry*, *410*, 177–188.

Miller, T. H., McEneff, G. L., Brown, R. J., Owen, S. F., Bury, N. R., & Barron, L. P. (2015). Pharmaceuticals in the freshwater invertebrate, *Gammarus pulex*, determined using pulverised liquid extraction, solid phase extraction and liquid chromatography–tandem mass spectrometry. *Science of the Total Environment*, *511*, 153–160.

Muschket, M., Di Paolo, C., Tindall, A. J., Touak, G., Phan, A., Krauss, M., Kirchner, K., Seiler, T. B., Hollert, H., & Brack, W. (2018). Identification of unknown antiandrogenic compounds in surface waters by effect-directed analysis (EDA) using a parallel fractionation approach. *Environmental Science & Technology*, *52*, 288–297.

Radke, M., Ulrich, H., Wurm, C., & Kunkel, U. (2010). Dynamics and attenuation of acidic pharmaceuticals along a river stretch. *Environmental Science & Technology*, *44*, 2968–2974.

Richter, M. K., Sander, M., Krauss, M., Christl, I., Dahinden, M. G., Schneider, M. K., & Schwarzenbach, R. P. (2009). Cation binding of antimicrobial sulfathiazole to leonardite humic acid. *Environmental Science & Technology*, *43*, 6632–6638.

Schmitt, M., Wack, K., Glaser, C., Wei, R., & Zwiener, C. (2021). Separation of photochemical and non-photochemical diurnal in-stream attenuation of micropollutants. *Environmental Science & Technology*, *55*, 8908–8917.

Schulze, T., Ahel, M., Ahlheim, J., Aït-Aïssa, S., Brion, F., Di Paolo, C., Froment, J., Hidasi, A. O., Hollender, J., Hollert, H., Hu, M., Kloß, A., Koprivica, S., Krauss, M., Muz, M., Oswald, P., Petre, M., Schollée, J. E., Seiler, T. B., … Brack, W. (2017). Assessment of a novel device for onsite integrative large-volume solid phase extraction of water samples to enable a comprehensive chemical and effect-based analysis. *Science of the Total Environment*, *581–582*, 350–358.

Schulze, T., Ricking, M., Schröter-Kermani, C., Körner, A., Denner, H. D., Weinfurtner, K., Winkler, A., & Pekdeger, A. (2007). The German Environmental Specimen Bank—Sampling, processing, and archiving sediment and suspended particulate matter. *Journal of Soils and Sediments*, *7*, 361–367.

Sébillot, A., Damdimopoulou, P., Ogino, Y., Spirhanzlova, P., Miyagawa, S., Du Pasquier, D., Mouatassim, N., Iguchi, T., Lemkine, G. F., Demeneix, B. A., & Tindall, A. J. (2014). Rapid fluorescent detection of (anti)androgens with spiggin-gfp medaka. *Environmental Science & Technology*, *48*, 10919–10928.

State Office for Flood Protection and Water Management Saxony-Anhalt. (2019). Datenportal Gewässerkundlicher Landesdienst Sachsen-Anhalt [Database state waterways service]. Stadt, Germany. Retrieved June 30, 2021, from https://gld-sa.dhi-wasy.de/GLD-Portal/

Ulrich, N., Endo, S., Brown, T. N., Watanabe, N., Bronner, G., Abraham, M. H., & Goss, K. U. (2017). UFZ-LSER database, Ver 3.2.1. Helmholtz Centre for Environmental Research–UFZ, Leipzig, Germany. Retrieved June 30, 2021, from https://www.ufz.de/lserd/

US Environmental Protection Agency. (2011). Definition and procedure for the determination of the method detection limit. 40 CFR 17 Part 136, Appendix B to Part 136 Revision 1.11. Washington, DC.

US Environmental Protection Agency. (2020). CPCat: Chemical and product categories. Washington, DC. Retrieved June 30, 2021, from https://actor.epa.gov/cpcat/faces/home.xhtml

Välitalo, P., Massei, R., Heiskanen, I., Behnisch, P., Brack, W., Tindall, A. J., Du Pasquier, D., Küster, E., Mikola, A., Schulze, T., & Sillanpää, M. (2017). Effect-based assessment of toxicity removal during wastewater treatment. *Water Research*, *126*, 153–163.

Weitere, M., Altenburger, R., Anlanger, C., Baborowski, M., Bärlund, I., Beckers, L.-M., Borchardt, D., Brack, W., Brase, L., Busch, W., Chatzinotas, A., Deutschmann, B., Eligehausen, J., Frank, K., Graeber, D., Griebler, C., Hagemann, J., Herzsprung, P., Hollert, H., … Brauns, M. (2021). Disentangling multiple chemical and non-chemical stressors in a lotic ecosystem using a longitudinal approach. *Science of the Total Environment*, *769*, Article 144324.

Writer, J. H., Antweiler, R. C., Ferrer, I., Ryan, J. N., & Thurman, E. M. (2013). In-stream attenuation of neuro-active pharmaceuticals and their metabolites. *Environmental Science & Technology*, *47*, 9781–9790.

Zhu, D., & Pignatello, J. J. (2005). A concentration-dependent multi-term linear free energy relationship for sorption of organic compounds to soils based on the hexadecane dilute-solution reference state. *Environmental Science & Technology*, *39*, 8817–8828.

